Estimating angular joint positions based on Electromyographic (EMG) activity

Xiangwei Meng, Teresa Zielenska, Eric Le Carpentier, Yannick Aoustin

Estimating angular joint positions based on Electromyographic (EMG) activity

Xiangwei Meng[1], Teresa Zielinska[2], Eric Le Carpentier[1], and Yannick Aoustin[1*]

***Abstract*— This study aims to estimate the movement of the upper limb using signals collected by surface electromyography (sEMG). Signals recorded for selected shoulder and elbow muscles during limb motion in the sagittal plane were used. An artificial neural network with fuzzy logic was applied to process sEMG signals. The network forecasts joint motion trajectories. These data are then used to determine joint torques based on inverse dynamics model. The angular trajectories obtained in dynamic simulation are compared with the real ones, allowing for the assessment of the motion estimation accuracy.**

I. INTRODUCTION

There are many people in the world with reduced mobility due to neuromuscular diseases. They need rehabilitation or motor support with the use of prostheses. For rehabilitation purposes, muscle signals from surface electrodes - sEMG - are often used, sometimes in combination with data recorded by the IMU. These data are used to forecast the intended movement [1], to estimate the movement itself [2]–[4] or to estimate driving torques [5]. In the case of robotic prostheses or exoskeletons with EMG control, it is important to analyze the features of EMG signals, [6], [7]. Many methods are used for this purpose. In this article, we apply a classification approach – an artificial neural network using fuzzy logic to determine joint motion trajectories of the upper limb when lifting weights. The sagittal plane is taken into account. Experimental results recorded for a human holding a 5 kg load in hand were used to train the network, and data for a 2 kg load were used for testing. The inverse dynamics model delivered joint driving torques based on the obtained trajectories. Dynamic simulation provided the angular trajectories compared with the real ones, allowing for assessing the motion estimation accuracy. The tests showed good prediction of joint torques for the elbow joint and worse prediction for the shoulder joint. The rest of the article is structured as follows. Chapter II discusses the biomechanics of the upper limb. The method of recording experimental data is presented in section III. sEMG processing and the use of a fuzzy logic artificial neural network to estimate shoulder and elbow trajectories are described in section IV. The numerical results are described in Sec. VI. The VII section presents conclusions and suggestions for further research.

[1]Xiangwei Meng, Eric Le Carpentier, and Yannick Aoustin are at Nantes Université, LS2N UMR CNRS 6004 1, rue de la Noë BP 92101 44321 NANTES Cedex 3, [1*]corresponding author: Yannick.Aoustin@univ-nantes.fr

[2] Teresa Zielinska is with Warsaw University of Technology, Faculty of Power and Aeronautical Engineering, Nowowiejska 24, 00-665 Warsaw teresa.zielinska@pw.edu.pl

II. BIOMECHANICS OF THE UPPER LIMB

A. Muscular system of the upper limb

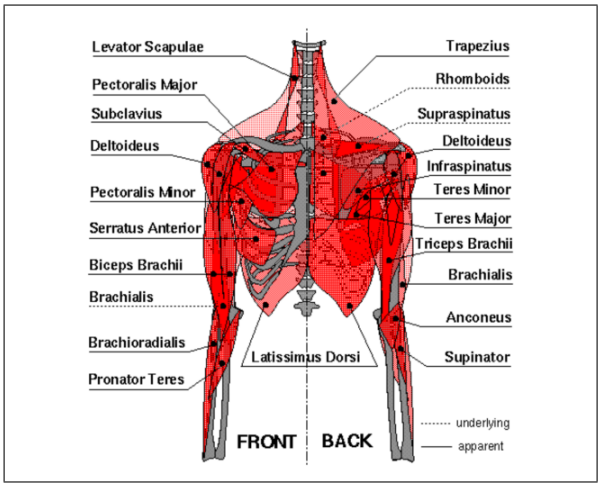

Fig. 1. The upper limb musculature [8].

Skeletal muscles play the role of actuators that drive body movement. The upper limb muscles are shown in Figure 1 [8]. A single muscle group typically contributes to more than one degree of freedom movement. In addition, typical movements usually require the coordinated effort of more than one muscle group to generate the required torque collectively. The relationship between movements and the upper limb muscles involved is presented in the Table I. Linking movements to the main muscle groups that drive them is a prerequisite for using sEMG signals to control the exoskeleton. This is due to the need to determine the appropriate arrangement of sensors recording sEMG signals. The shoulder joint is a complex structure capable of performing omnidirectional movements. Conversely, the elbow is a hinge joint because it flexes and straightens like a hinge. The next degree of freedom is located where the radius meets the humerus, allowing the hand to move up and down.

B. Anthropometric data of the upper limb

The computation of the mass and the location of the center of mass (COM) from the proximal joint is based on the paper limb data. The knowledge about the subject gender, body mass and height allows us to take the anthropometric data of the upper limb – see Table II. Considering the personal variations in body dimensions for each subject, the mass and length of each segment and the center of mass are represented as percentages of the total body mass and height and corresponding segment length, respectively.

TABLE I

UPPER LIMB MOVEMENTS AND THEIR RELATED MUSCLES (KENHUB)

Joints	Movements	Muscles
Shoulder	Flexion	Pectoralis major Anterior deltoid Coracobrachialis
	Extension	Posterior deltoid Latissimus dorsi Teres major
	Abduction	0-15 degrees: Supraspinatus 15-90 degrees: Middle deltoid Past 90 degrees: Trapezius and Serratus anterior
	Adduction	Pectoralis major Latissimus dorsi Teres major
	Internal rotation	Subscapularis Pectoralis major Latissimus dorsi Teres major Anterior deltoid
	External rotation	Infraspinatus Teres minor
Elbow	Flexion	Biceps brachii Brachialis Brachioradialis
	Extension	Triceps brachii Anconeus
	Pronation	Pronator quadratus Pronator teres
	Supination	Supinator

TABLE II

ANTHROPOMETRIC DATA OF THE UPPER LIMB REPRESENTED AS PERCENTAGES [9], [10]

Segment	Mass/ Total mass	Length/ /Total height	COM/ Segment length
Upper arm	2.8%	18.8%	46.1%
Forearm and hand	1.6%+0.6%	14.5%+10.8%	67.7%*

C. A simplified kinematic model of the upper limb

It was chosen to base this work on a simplified model of the upper limb, which consists of two parts – the upper arm and the forearm with two joints – the shoulder and the elbow, with one degree of freedom (DoF) each (Fig. 2). The body

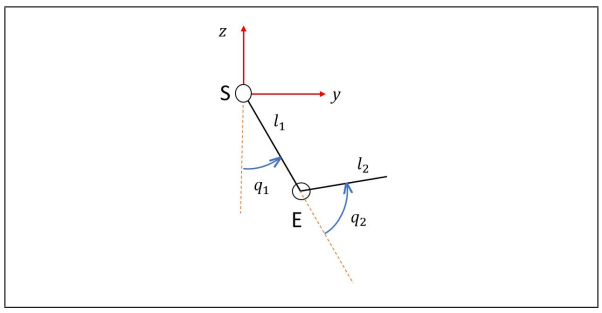

Fig. 2. Simplified kinematic model.

reference frame is attached to the center of the shoulder (S). Parameters l_1 and l_2 are the lengths of the upper arm and the forearm respectively. The joint variables, q_1 and q_2, represent the shoulder and elbow rotation around the x-axis, meaning the flexion/extension motion. Therefore, these simplifications lead to describing the dynamic model of the upper limb as follows.

$$\mathbf{D}(\mathbf{q})\ddot{\mathbf{q}} + \mathbf{C}(\mathbf{q},\dot{\mathbf{q}}) = \Gamma \tag{1}$$

Here $\mathbf{q} = (q_1, q_2)^\top$, $\mathbf{D}(\mathbf{q})(2\times 2)$ is a symmetric positive definite inertia matrix, $\mathbf{C}(\mathbf{q},\dot{\mathbf{q}})(2\times 1)$ is a vector, which groups the centrifugal, Coriolis, and gravity forces. Vector $\Gamma(2\times 1)$ groups the joint torques applied in the shoulder and elbow.

III. DATASET

The Warsaw Children's Memorial Hospital provides the dataset used in this work. It consists of twelve trials in which a healthy male adult subject performs the flexion/extension motion of the elbow, holding different loads in the hand. The experimental protocol involving the adult subject complies with the Declaration of Helsinki. The whole data set included the results with 0, 1, 2, and 5 kg load kept in hand; however, in this research, we considered the data for 2 and 5 kg only. The trials were arranged in three groups of four trials each, depending on the subject's position. In the first group, the subject stands on one force platform while recording the motion. He stands on two platforms in the second group, while in the third group, he is seated. The dataset includes the sEMG data recorded from 16 channels attached to the main muscles of the upper limb. Additionally, the positions and the angles of the whole body were recorded with a camera featuring a large number of optical sensors. Each of these sensors is associated with one of the optical markers attached to the subject. The sEMG data were automatically pre-processed: the signals were amplified to $0-5$V and filtered to reduce the noise. It was chosen to use the data from the channels, where their electrodes were located above the main muscle group that contracts more intensively during the performance of the designed movements. The data were recorded using the VICON system with the dedicated software. Besides research purposes, the hospital uses the system to diagnose children's neural diseases and test rehabilitation and medication processes. The VICPON software also delivered the torques, which are calculated using the anthropometric data of the person. There are also two force platforms for measuring the support reaction.

IV. SEMG PROCESSING AND FEATURE EXTRACTION

Before using it in training and testing processes, the sEMG data were processed. As in [3] any direct current (DC) component is first removed from the sEMG signals using a six-order zero-phase Butterworth high pass filter at the cutoff frequency of 1 Hz, on account of the frequency of DC component being 0 Hz. After that, the sEMG signals were full-wave rectified to obtain absolute value and next, they were low-pass filtered at 2 Hz with a sixth-order zero-phase Butterworth filter, to produce a linear envelope, that is, to preserve the inherent variation of the sEMG signal characteristics. The selected features used for farther processing are the root mean square (RMS) and the maximum fractal length (MFL), obtained using a software package developed in Matlab by Too *et al* [11]. The RMS characterizes the magnitude of the signal: it represents the effective value of the electrical signal – a measure of the signal power. It is

computed as follows:

$$RMS = \sqrt{\frac{1}{N}\sum_{i=1}^{N} x_i^2} \tag{2}$$

in which x_i is the $i-$th value of the sEMG signal x of a segment and N is the number of samples in a segment. MFL was proposed by Arjunan et al. [12] to measure low-level muscle activation and contraction strength.

$$MFL = \log_{10}\left(\sqrt{\sum_{i=1}^{N-1}(x_{i+1}-x_i)^2}\right) \tag{3}$$

The literature indicates MFL it is very similar to the waveform length expressed in the logarithmic scale; thus, it is less noise-sensitive.

V. Estimation Of An Upper Limb Motion Using sEMG

An artificial neural network estimates the elbow and shoulder trajectories using fuzzy logic that processes the recorded sEMG signals. According to the biomechanics of the upper limb presented in Sec. II, the muscle group related to elbow flexion and extension movements comprises Biceps Brachii, Brachioradialis and Triceps Brachii, and the only muscle associated with shoulder flexion and extension motions is the Deltoid.

A. Fuzzy Inference System

An adaptive network using fuzzy logic was implemented in such a way that, based on the processed sEMG signals, it was able to estimate the intended angular position, with the inputs RMS and the MFL, Fig. 3. The fuzzy inference

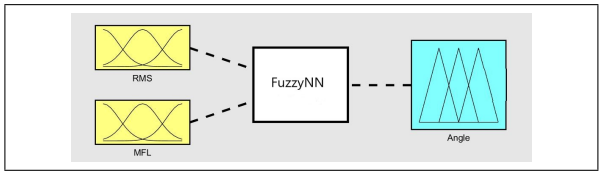

Fig. 3. Estimating the intended angular position with an adaptive network using fuzzy logic.

system (FIS) is the key unit of a fuzzy logic system that enables decision making. Fuzzy logic is used in control systems, pattern recognition, decision making, etc. Also in the processing and classification of biological signals, fuzzy logic works very well because biological signals are not fully repeatable and the information they carry is not always unambiguous. [13]. Among the best-known fuzzy inference systems (FIS) is Mamdani's, [14] with the principles shown in Fig. 4. With two inputs and one output, the rules are as follows:

- If x is A_1 and y is B_1, then z is C_1
- If x is A_2 and y is B_2, then z is C_2

FIS includes the fuzzification step that links the inputs x and y to a fuzzy set $\mathrm{A}_i, \mathrm{B}_i$ via membership functions, the inference step that calculates a firing strength f_i as the product of the outputs from the first layer, for each rule according to the fuzzy operator, the implication step, applies the rule weight W_i to f_i and reshapes the membership function of output fuzzy set C_i for each rule according to the implication operator, the aggregation step that combines the implied fuzzy sets of all rules into a single fuzzy set according to the aggregation operator and the defuzzification step that uses a defuzzification method to calculate a crisp output from the aggregated result. Mamdani FIS has the advantage that it is intuitive and well adapted to the human way of reasoning, therefore it is readable and understandable to us.

The Mamdani-type FIS used in this work was designed using the Fuzzy Logic Designer MATLAB toolbox®. The relationship between the angle of joint flexion and extension and the features of sEMG is not linear. As a consequence, the membership function of input fuzzy sets is set as a Gaussian function, which is derived from Gaussian distribution, expressed as follows

$$f(x;\sigma,c) = \exp\left(\frac{-(x-c)^2}{2\sigma^2}\right) \tag{4}$$

where σ is the standard deviation and c is the mean for the Gaussian function. $[\sigma,\ c]$ is the parameter set for the fuzzy set. The output space is assigned into three fuzzy sets, low, medium, and high, representing the range of the joint motion, which is low, medium, and high, respectively. The range of output is determined based on the dataset. The membership function of output fuzzy sets is also chosen as a Gaussian function.

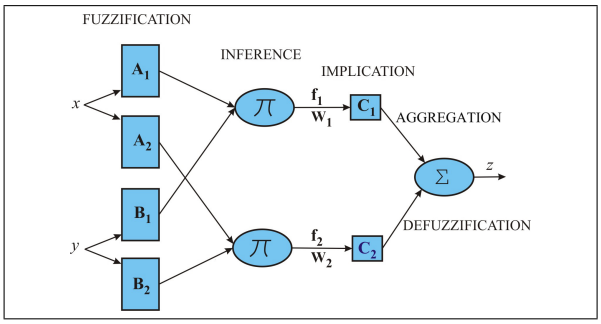

Fig. 4. A general model of Mamdani FIS.

B. Estimation of the elbow joint trajectory

Tables III and IV give for the three fuzzy sets, low, medium, and high, $[\sigma,\ c]$ for the Gaussian function or $[\sigma_1,\ \sigma_2,\ c_1,\ c_2]$ for Gaussian2 function. The relationships between the inputs and the output are defined through the "IF-THEN" rules:

1) If (RMS-BI is low) and (MFL-BI is low) then (angle is low) (1)
2) If (RMS-BI is med) and (MFL-BI is low) then (angle is med) (0.5)
3) If (RMS-BI is high) and (MFL-BI is high) then (angle is high) (1)
4) If (RMS-BI is low) and (MFL-BI is high) then (angle is med) (1)
5) If (RMS-BI is med) and (MFL-BI is high) then (angle is high) (0.5)

TABLE III

PARAMETERS OF THE MEMBERSHIP FUNCTIONS IN ELBOW'S FIS (BI-BICEPS BRACHII, BRA-BRACHIORADIALIS, TRI-TRICEPS BRACHII)

Name of the membership functions		"low" fuzzy set	"med" fuzzy set	"high" fuzzy set
Input	RMS-BI	[0.07984, 0, 0.07984, 0.156]	[0.065, 0.5026]	[0.073, 0.85, 0.073, 1]
	MFL-BI	[0.13, 0.2, 0.13, 0.5]		[0.045, 0.9, 0.045, 1]
	RMS-BRA	[0.07, 0, 0.07, 0.17]	[0.06, 0.49]	[0.08, 0.88, 0.08, 1]
	MFL-BRA	[0.102, 0.17, 0.102, 0.574]		[0.0294, 0.9, 0.0294, 1]
	RMS-TRI	[0.0891, 0.2483]		[0.08, 0.637, 0.08, 0.9]
	MFL-TRI	[0.12, 0.3353]		[0.1, 0.86]
Output	Angle	[9, 21]	[5.1, 50]	[15.6, 104]

6) If (RMS-BRA is low) and (MFL-BRA is low) then (angle is low) (0.5)
7) If (RMS-BRA is med) and (MFL-BRA is low) then (angle is med) (0.5)
8) If (RMS-BRA is high) and (MFL-BRA is high) then (angle is high) (0.5)
9) If (RMS-BRA is low) and (MFL-BRA is high) then (angle is med) (0.5)
10) If (RMS-BRA is med) and (MFL-BRA is high) then (angle is high) (0.5)
11) If (RMS-BI is low) and (MFL-BI is low) and (RMS-TRI is high) and (MFL-TRI is high) then (angle is low) (1)
12) If (RMS-BI is med) and (MFL-BI is low) and (RMS-TRI is high) and (MFL-TRI is high) then (angle is low) (1)

The numbers given in parentheses at the end of each mainline represent the weight of each rule, ranging from 0 to 1.

C. Estimation of the shoulder joint trajectory

TABLE IV

PARAMETERS OF THE MEMBERSHIP FUNCTIONS IN SHOULDER'S FIS

Name of the membership functions		"low" fuzzy set	"med" fuzzy set	"high" fuzzy set
Input	RMS	[0.05, 0.128]	[0.075, 0.41]	[0.0859, 0.8009]
	MFL	[0.0543, 0.1358]	[0.0922, 0.4433]	[0.085, 0.8]
Output	Angle	[3.091, -14.57]	[3.58, 0.5]	[4.286, 17.48]

Since Deltoid has a positive relation with shoulder flexion, the "IF-THEN" rules are similar to those of Biceps Brachii in elbow prediction, illustrated as following, along with the weight of this rule in the last pair of parentheses:

1) If (RMS is low) and (MFL is low) then (angle is low) (1)
2) If (RMS is low) and (MFL is med) then (angle is low) (1)
3) If (RMS is low) and (MFL is high) then (angle is med) (1)
4) If (RMS is med) and (MFL is low) then (angle is low) (1)
5) If (RMS is med) and (MFL is med) then (angle is med) (1)
6) If (RMS is med) and (MFL is high) then (angle is high) (1)
7) If (RMS is high) and (MFL is low) then (angle is med) (1)
8) If (RMS is high) and (MFL is med) then (angle is high) (0.5)
9) If (RMS is high) and (MFL is high) then (angle is high) (1)

VI. RESULTS

In the study presented here, the choice was made to use arm movements only when the subject stands upon one force platform. Each movement recorded for training or testing phases leads to a data vector comprising 1100 samples. The parameter N for calculating RMS and MFL is equal to 100.

A. Training phase: Estimation of the shoulder and elbow angles and determination of the corresponding joint torques

The data used for the training phase corresponded to the case when the subject with a hand load of 5 kg. The obtained output signals of FIS were not so smooth. Therefore, these outputs were filtered to obtain the estimates of real angles for the shoulder and the elbow. Furthermore, it was observed that there is a time difference between the estimated and measured angles. Actually, this kind of time delay has been presented and observed in previous studies [15], [16]. It is known as the electromechanical delay, between the onset of the EMG signals and the exerting muscles' tension. The electromechanical delay can vary depending on many factors such as different intended tasks, muscle shortening velocity, degree of fatigue and type of muscle fibre [17]. FIS training outputs after filtering are shown in Fig. 5 for the shoulder and in Fig. 6 for the elbow. In Fig. 5 the output of FIS (red curve) follows a similar trend with the actual angle (blue curve), but it fluctuates wildly, especially during the first two seconds. The main reason is that the shoulder joint is much more complex than the elbow joint, and it is more difficult to achieve a good prediction accuracy. In addition, precise shoulder angular trajectory prediction is more complicated to implement due to the available shoulder motion record in the dataset being very limited. Moreover, another possible reason is that the transient state when the muscle goes from rest to contraction level, is more difficult to classify accurately than the steady state during a constantly maintained contraction in muscle [18]. The great fluctuation during the first two seconds indeed lies in the period when the transition between transient state and steady state occurs. In Fig. 6 (elbow), the estimated angle (red curve) shares a similar trend with the actual angle (blue curve) to an acceptable extent. The

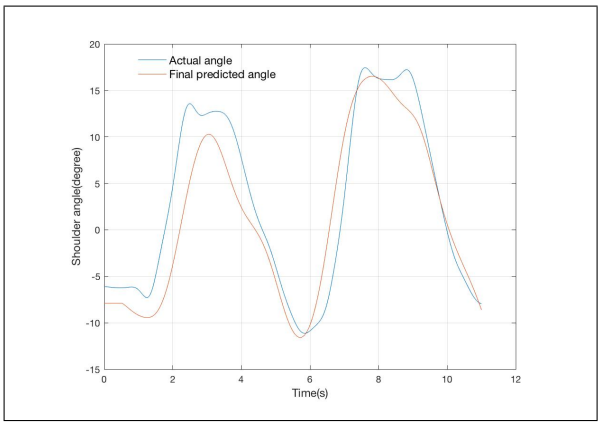

Fig. 5. Training phase: Measured (blue curve) and estimated joint angle result of FIS (red curve) in the shoulder.

estimated shoulder and elbow angles are applied as the generalized coordinates q_1 and q_2 of the vector $\mathbf{q}$ in the dynamic model expressed by equation (1). The generalized velocities $\dot{\mathbf{q}}$ and accelerations $\ddot{\mathbf{q}}$ were calculated using the Euler discretization method. Knowing vectors $\mathbf{q}$, $\dot{\mathbf{q}}$, $\ddot{\mathbf{q}}$ and the dynamical parameters allowed us to determine the left side terms in equation (1) and the calculation of the joint torque

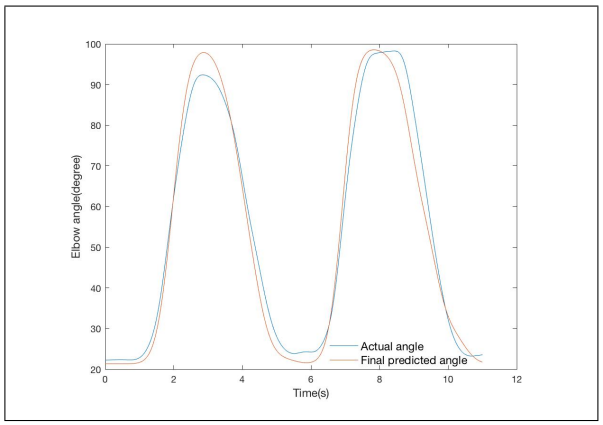

Fig. 6. Training phase: Measured (blue curve) and estimated joint angle result of FIS (red curve) in the elbow.

vector Γ. Figs 7 and 8 are presenting that the estimated joint angles and the calculated torques of the shoulder and the elbow are following their corresponding real trajectories and torques with some small discrepancies during the entirety of the time range. It is also noted that, at the beginning and in the minima area, the estimated torque is about 1 Nm bigger than the real torque. The reasons for these discrepancies are the inherent inaccuracies in the joint trajectories estimation and the simplifications introduced to the dynamic model (1).

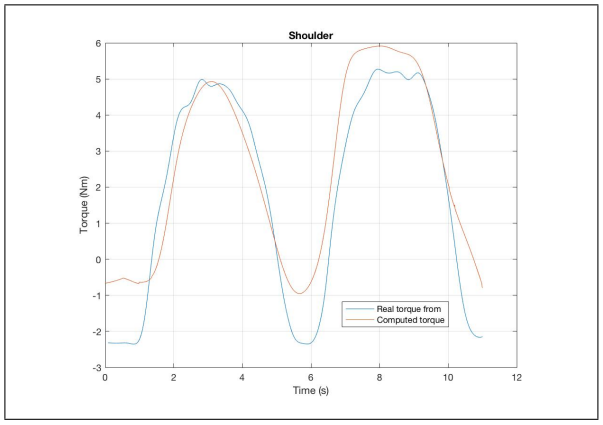

Fig. 7. Training phase: Measured (blue curve) and calculated (red curve) torques in the shoulder.

B. Testing phase: Estimation of the shoulder and elbow angles and determination of the corresponding joint torquess

For the testing phase, the used data correspond to the case where the subject stands upon one force platform with a hand load of 2 kg. The testing outputs of FIS after filtering are shown in Fig. 9 for the shoulder and in Fig. 10 for the elbow. The generalized velocities $\dot{\mathbf{q}}$ and accelerations $\ddot{\mathbf{q}}$ were calculated using the Euler discretization method. Similarly to the training phase, the joint torque vector Γ was calculated and compared with the measured torques for the shoulder Fig. 11 and the elbow Fig. 12. The discrepancies encountered during the training phase for shoulder torque are «amplified» using the test data. On the other hand, the results for the

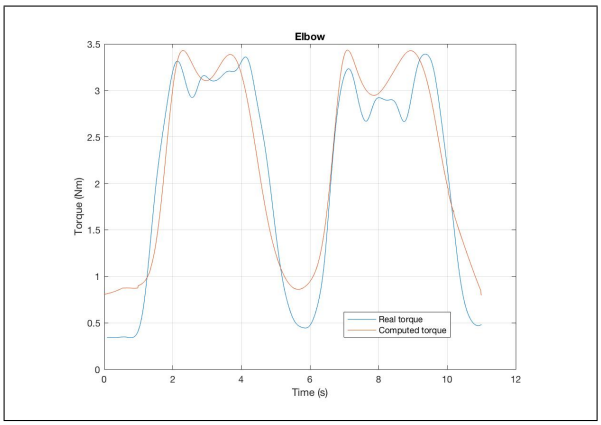

Fig. 8. Training phase: Measured (blue curve) and calculated (red curve) torques in the elbow.

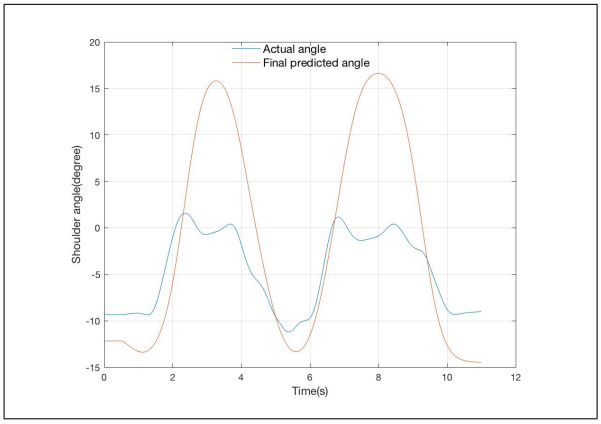

Fig. 9. Testing phase: Measured (blue curve) joint angle and estimated (red curve) joint angle result of FIS in the shoulder.

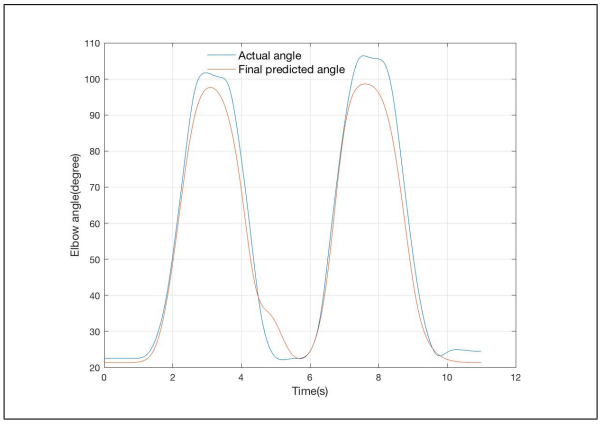

Fig. 10. Testing phase: Measured (blue curve) joint angle and estimated joint angle result of FIS (red curve) in the elbow.

elbow remain good. Besides model simplifications, this may be explained by less precise measurement of muscle activity at the shoulder.

VII. CONCLUSIONS

The artificial neural network using fuzzy logic gives satisfactory results in estimating the joint variable of the elbow. The results are less accurate for the case of the shoulder. It is necessary to use other classification algorithms that may

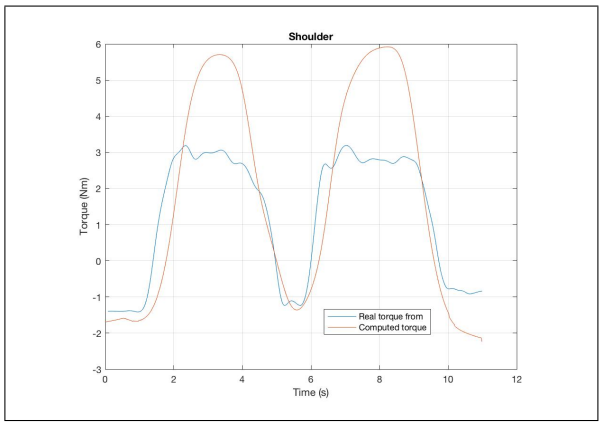

Fig. 11. Testing phase: Measured (blue curve) and calculated (red curve) torques in the shoulder.

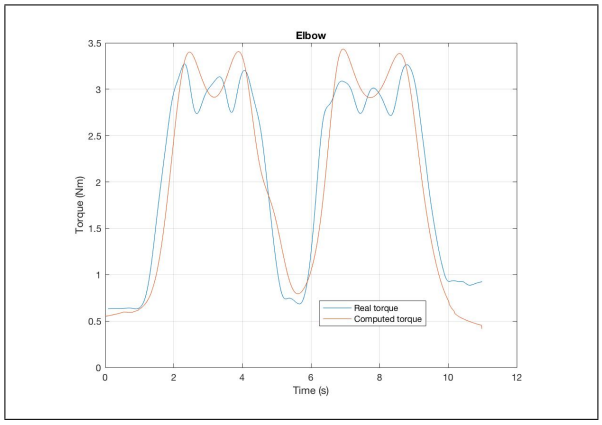

Fig. 12. Testing phase: Measured (blue curve) and calculated (red curve) torques in the elbow.

consider more sEMG features. In the long term, this study is focused on using exoskeletons for upper limbs, helping patients suffering from neuropathy or myopathy to when performing daily tasks. Therefore, preserving the motion ability of the upper part of their body becomes crucial to maintaining their mobility and daily activities.

ACKNOWLEDGMENT

We would like to express our gratitude to the Cluster Frame (https://next-isite.fr/frame) for supporting the project and to Professor Malgorzata Syczewska and the Kinesiology Laboratory, Department of Rehabilitation of The Children's Memorial Health Institute in Warsaw for sharing the motion recording infrastructure and professional support offered during data collecting. Warsaw University of Technology, Faculty of Power and Aeronautical Engineering - Doctor Marek Surowiec made the collected data available.

REFERENCES

[1] N. Petranon and S. Umchid, "Design and development of hand movement detection device for sign language using imu and semg sensors," in *2023 Research, Invention, and Innovation Congress: Innovative Electricals and Electronics (RI2C)*, 2023, pp. 1–4.

[2] J. Too, A. R. Abdullah, and N. M. Saad, "Classification of hand movements based on discrete wavelet transform and enhanced feature extraction," *International Journal of Advanced Computer Science and Applications*, vol. 10, no. 6, 2019. [Online]. Available: http://dx.doi.org/10.14569/IJACSA.2019.0100612

[3] R. Tibold and A. Fuglevand, "Prediction of muscle activity during loaded movements of the upper limb," *Journal of NeuroEngineering and Rehabilitation*, vol. 12, no. 1, p. 6, 2015. [Online]. Available: https://doi.org/10.1186/1743-0003-12-6

[4] A. Au and R. Kirsch, "Emg-based prediction of shoulder and elbow kinematics in able-bodied and spinal cord injured individuals," *IEEE Transactions on Rehabilitation Engineering*, vol. 8, no. 4, pp. 471–480, 2000.

[5] S. P. Sitole and F. C. Sup, "Continuous prediction of human joint mechanics using emg signals: A review of model-based and model-free approaches," *IEEE Transactions on Medical Robotics and Bionics*, vol. 5, no. 3, pp. 528–546, 2023.

[6] T. Zielinska, J. Wang, W. Ge, and L. Lyu, "Comparative study of muscles effort during gait phases for multi-muscle humanoids," in *2019 12th International Workshop on Robot Motion and Control (RoMoCo)*, 2019, pp. 62–67.

[7] L. B. and A. C., "Feasibility study of upper limb control method based on electromyography-angle relation," *Journal of Computational and Nonlinear Dynamics*, vol. 18, no. 6, p. 064501, 2023.

[8] K. Veer and R. Agarwal, "Wavelet and short-time fourier transform comparison-based analysis of myoelectric signals," *Journal of Applied Statistics*, vol. 42, no. 7, pp. 1591–1601, 2015. [Online]. Available: https://doi.org/10.1080/02664763.2014.1001728

[9] D. Winter, *Anthropometry. In Biomechanics and Motor Control of Human Movement*. Wiley, 2009. [Online]. Available: https://doi.org/10.1002/9780470549148.ch4

[10] R. Contini, R. J. Drillis, and M. Bluestein, "Determination of body segment parameters," *Human Factors*, vol. 5, no. 5, pp. 493–504, 1963, pMID: 14101572. [Online]. Available: https://doi.org/10.1177/001872086300500508

[11] J. Too, A. Rahim, and N. Mohd, "Classification of hand movements based on discrete wavelet transform and enhanced feature extraction," *Int. J. of Advanced Computer Science and Applications*, vol. 10, no. 6, 2019. [Online]. Available: https://doi.org/10.145692Fijacsa.2019.0100612

[12] S. P. Arjunan and D. K. Kumar, "Decoding subtle forearm flexions using fractal features of surface electromyogram from single and multiple sensors," *Journal of NeuroEngineering and Rehabilitation*, vol. 7, no. 1, p. 53, 2010. [Online]. Available: https://doi.org/10.1186/1743-0003-7-53

[13] R. Suppiah, N. Kim, K. Abidi, and A. Sharma, "Bio-inspired fuzzy inference system—for physiological signal analysis," *IET Cyber-Systems and Robotics*, vol. 5, no. 3, p. e12093, 2023. [Online]. Available: https://ietresearch.onlinelibrary.wiley.com/doi/abs/10.1049/csy2.12093

[14] E. Mamdani and S. Assilian, "An experiment in linguistic synthesis with a fuzzy logic controller," *International Journal of Man-Machine Studies*, vol. 7, no. 1, pp. 1–13, 1975. [Online]. Available: https://www.sciencedirect.com/science/article/pii/S0020737375800022

[15] N. A. Shrirao, N. P. Reddy, and D. R. Kosuri, "Neural network committees for finger joint angle estimation from surface emg signals," *BioMedical Engineering OnLine*, vol. 8, no. 1, p. 2, 2009. [Online]. Available: https://doi.org/10.1186/1475-925X-8-2

[16] J. G. Ngeo, T. Tamei, and T. Shibata, "Continuous and simultaneous estimation of finger kinematics using inputs from an emg-to-muscle activation model," *Journal of NeuroEngineering and Rehabilitation*, vol. 11, no. 1, p. 122, 2014. [Online]. Available: https://doi.org/10.1186/1743-0003-11-122

[17] T. S. Buchanan, D. G. Lloyd, K. Manal, and T. F. Besier, "Neuromusculoskeletal modeling: estimation of muscle forces and joint moments and movements from measurements of neural command," *Journal of applied biomechanics*, vol. 20, no. 4, pp. 367–395, 2004. [Online]. Available: https://doi.org/10.1123/jab.20.4.367

[18] M. Asghari Oskoei and H. Hu, "Myoelectric control systems—a survey," *Biomedical Signal Processing and Control*, vol. 2, no. 4, pp. 275–294, 2007. [Online]. Available: https://www.sciencedirect.com/science/article/pii/S1746809407000547